ELSEVIER

Journal of Nuclear Materials 289 (2001) 254–262

journal of nuclear materials

www.elsevier.nl/locate/jnucmat

Kinetics of uranium release from Synroc phases

Y. Zhang [a,*], K.P. Hart [a], W.L. Bourcier [b], R.A. Day [a], M. Colella [a], B. Thomas [a], Z. Aly [a], A. Jostsons [a]

[a] *Australian Nuclear Science and Technology Organisation, Private Mail Bag 1, Menai, NSW 2234, Australia*
[b] *Lawrence Livermore National Laboratory, Livermore, CA 94550, USA*

Received 21 September 2000; accepted 3 January 2001

Abstract

This paper presents experimental studies on the kinetics of U release from near single-phase zirconolite, pyrochlore, brannerite and pyrochlore-rich titanate ceramic materials. The dissolution tests were conducted at 20–75°C with initial pHs from 2 to 12, and flow rates from 10 to 80 ml d^{-1} in the open atmosphere. The U releases from these titanate materials are controlled by initial fast process and then followed by linear kinetics. The close-to-stoichiometric U release from zirconolite and pyrochlore-rich materials and preferential U release from brannerite are consistent with the alterations observed for the natural samples. The rate constants for U releases were determined and the effects of pH and temperature were examined. For each material, the U release vs. pH exhibits a V-shape with a minimum near pH 8. The measured activation energies suggest surface reaction controlled dissolution mechanism. Pyrochlore-rich materials and zirconolite demonstrated higher chemical durability and more resistance to aqueous attack than brannerite. However, impurities and minor brannerite inclusions do not appear to have a detrimental effect on U releases from pyrochlore-rich multi-phase ceramics. © 2001 Elsevier Science B.V. All rights reserved.

1. Introduction

Synroc, a titanate-based ceramic, has received consideration as a matrix for immobilisation of actinide-rich radioactive wastes [1–3]. In the last 10 years two actinide-bearing titanate phases, zirconolite ($CaZrTi_2O_7$) and pyrochlore (nominally $CaATi_2O_7$, A-actinide elements), have been extensively studied [4–7]. Ceramic formulations based on these two phases have also been developed for immobilisation of excess Pu [8,9]. Brannerite, UTi_2O_6, has been identified as a minor phase in some of these formulations [10,11].

Aqueous durability studies on these ceramic formulations and individual Synroc phases, largely based on the standard MCC-1 leaching tests, have been performed to support the development of the formulations [12,13].

To evaluate the long-term durability of the ceramic products and each individual Synroc phase, some thermodynamic and kinetic information is essential, including a definition of the mechanism of the dissolution process, kinetics of actinide releases, and the development of a mathematical description of the dissolution process. In addition, a comparison with natural minerals is essential.

This paper reports experimental studies on the kinetics of U releases from the pyrochlore-rich formulations and near single-phase zirconolite, pyrochlore and brannerite, and evaluates parameters for the further mathematic modelling to predict the long-term stability of these materials.

2. Experimental

2.1. Sample preparation

The ceramic materials used in this study are based on the selected composition [9] for immobilisation of

---

[*] Corresponding author: Fax: +61-2 9543 7179.
E-mail address: yzx@ansto.gov.au (Y. Zhang).

PII: S0022-3115(01)00423-8

surplus Pu. Depleted uranium was used for all sample preparation. The Pu consisted of mainly ^{239}Pu with small amounts of ^{240}Pu (~5 wt%) and trace amounts of ^{241}Pu and ^{241}Am.

Brannerite was prepared by using the alkoxide/nitrate route [10]. Stoichiometric mixtures of aqueous uranyl nitrate and ethanolic Ti isopropoxide solutions were dried and calcined in argon at 750°C for 1 h. The calcines were wet-milled for 2 h and then dried. Two wt% of Ti metal was added and samples were hot-pressed at 1260°C for 2 h under 21 MPa in graphite dies. The sample contains mainly brannerite with ~5–7% of rutile and trace amounts of UO_2.

Zirconolite and pyrochlore-rich materials were prepared via oxide route [14]. Typical grain size ranges from 5–50 μm. The ceramic formulations, sintering recipes and oxide compositions are given in Tables 1 and 2.

The monolithic samples were crushed and sieved to 75–150 μm for brannerite and 20–40 mm for the others, and washed with acetone to remove the fines. The surface areas were measured by the BET method as around 0.2 $m^2\ g^{-1}$ for 20–40 μm and 0.08 $m^2\ g^{-1}$ for 75–150 μm.

2.2. Electron microscopy

Scanning electron microscopy (SEM) was carried out with a JEOL 6400 instrument operated at 15 kV, and fitted with a Noran Voyager IV X-ray microanalysis System (EDX). Calibrations for microanalysis were carried out using a comprehensive set of standards for quantitative analysis [8,15]. Transmission electron microscopy (TEM) was carried out with a JEOL 2000FXII equipped with a Link-ISIS EDX system, operated at 200 kV and calibrated for quantitative thin-film analyses using an extensive set of natural and synthetic reference materials [15].

2.3. Test method

Dissolution tests (Single-Pass-Flow-Through), using methods described elsewhere [16,17], were conducted at 20–75°C using solutions with initial pHs from 2 to 12 and flow rates from 10 to 80 ml d^{-1} in an open atmosphere, i.e. in equilibrium with the laboratory atmosphere. A varying flow rate was used for each individual test for Ce–U (~18–45 ml d^{-1}), Pu–U (~15–60 ml d^{-1}) ceramics, zirconolite (~40–80 ml d^{-1}) and pyrochlore (~40–80 ml d^{-1}). For brannerite, a constant flow rate (10–30 ml d^{-1}) was used. The chemical compositions of the leachants are given in Table 3. The powdered sample was placed between Teflon membranes, held together by two Teflon rings, and positioned near the middle of the Teflon leaching vessel. The leachates were collected twice per week and were acidified after pH measurement with 3% by volume of analytical grade HNO_3. Inductively coupled plasma mass spectrometry (ICP–MS) was used to determine the concentrations of U and Ti in the leachates. The powdered specimens, after dissolution tests, were gently rinsed with deionised water and dried

Table 1
Ceramic formulations

Sample	Precursor	Generic composition description	Preparation conditions
Ce–U baseline	Oxide	Pyrochlore-rich + zirconolite + rutile + brannerite	Sintered at 1350°C in air
Pu–U impurity	Oxide	Pyrochlore-rich + zirconolite + rutile + brannerite	Sintered at 1350°C in air
Pyrochlore	Oxide	>95% + rutile+ brannerite	Sintered at 1350°C in air
Zirconolite	Oxide	only a little rutile	Sintered at 1350°C in air
Brannerite	Alkoxide	>93%, ~5% TiO_2 (rutile) + ~2% Ti	HIPed at 1260°C in air

Table 2
Sintering recipes (oxide weight for 50 g batch) and oxide compositions (wt%) of ceramic materials used in the dissolution tests

	Zirconolite		Pyrochlore		Brannerite	Ce–U ceramic		Pu–U ceramic	
	grams	wt%	grams	wt%	wt%	grams	wt%	grams	wt%
CaO	8.03	9.68	8.64	10.48	–	7.98	12.56	4.95	9.9
CeO_2	2.96	6.37	3.89	8.43	–	4.63	9.64	–	–
Ga_2O_3	–	–		–	–	–	–	0.07	0.14
Gd_2O_3	3.22	6.92	3.75	8.13	–	–	–	3.95	7.9
HfO_2	11.80	25.38	5.78	12.51	–	5.67	11.79	5.30	10.6
MgO	–	–	–	–	–	–	–	0.01	0.02
PuO_2	–	–	–	–	–	–	–	5.95	11.9
TiO_2	16.49	35.49	16.73	36.20	38.8	17.19	35.77	17.95	35.9
UO_2	7.50	16.15	11.20	24.25	60.1	14.53	30.24	11.80	23.6
ZnO	–	–	–	–	–	–	–	0.06	0.11

Table 3
Composition of leachants

Composition	Initial pH
0.05 M KHphthalate + 0.05 M HCl	2.1
0.05 M KHphthalate + 0.03 M HCl	3.0
0.05 M KHphthalate + 0.015 M HCl	4.1
0.05 M KHphthalate + 0.04 M NaOH	5.6
0.05 M H_3BO_3 + 0.004 M NaOH	7.9
0.05 M H_3BO_3 + 0.044 M NaOH	9.8
0.05 M KCl + 0.012 M NaOH	11.9

at the test temperature for SEM and TEM examinations. The dissolution tests for brannerite were carried out at ANSTO and the rest were carried out at LLNL.

3. Results

3.1. General observations

The normalised U/Ti mole ratios leached in the pH 2.1 buffer solution are shown as a function of time in Fig. 1. The results indicate that the U release from brannerite is non-stoichiometric (with respect to Ti) but U release from the other materials is close to stoichiometric after about 20 days.

Two flow patterns were used, constant flow rate and varying flow rate, to evaluate the effect of flow rate on U releases. For Ce–U, Pu–U, zirconolite and pyrochlore, a varying flow rate (15–80 ml d^{-1}) was used for each individual test. The normalised U release rates are nearly independent of the varying flow rate, implying that the U releases are not solubility-controlled [14]. For brannerite, constant flow rates were used, and flow rate variation by a factor of 3 (10–30 ml d^{-1}) had no obvious effects on the normalised U release rates.

3.2. Kinetics

The typical cumulative U releases from Ce–U and Pu–U ceramics, zirconolite, pyrochlore and brannerite are shown in Figs. 2–6. The U releases are controlled by initial fast process and followed by linear kinetics (steady state release). The later linear part of the plot of cumulative U release vs. time has been used to calculate the limiting rate constant. The fitted limiting rate constants for U releases are summarised in Table 4.

3.3. Surface analysis

SEM examination of the powdered Ce–U (pyrochlore-rich) ceramic after dissolution tests in the pH 2.1 solution at 25°C for one year (not shown) indicates that the reacted sample appears to be identical to the unreacted and there is no obvious rounding or smoothing of edges and pits (note-images on 30-μm scale), which is in agreement with the thickness of the surface alteration layer of 4 nm calculated from the U release data [14].

SEM examination of the powdered brannerite samples after leaching at 70°C for more than 98 days [19] revealed that the major surface alteration product is TiO_2 and the alteration thickness ranges from tens to hundreds of nanometres. Different surface morphologies, i.e. a near uniform film under acidic leaching (Fig. 7(a)), in contrast to ~50–100 nm-sized spherules under alkaline leaching (Fig. 7(b)), were identified.

TEM observations on the reacted brannerite samples clearly defined the two kinds of surface morphologies, viz. nearly uniform films (anatase-TiO_2) in acidic media (Fig. 8(a)) and plate-like crystallite TiO_2 (anatase) in alkaline media (Fig. 8(b)).

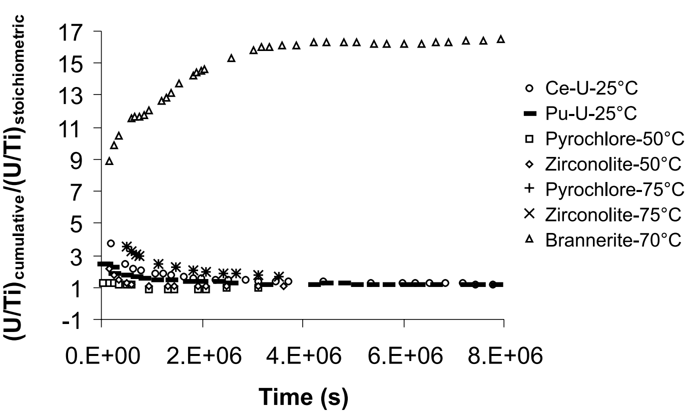

Fig. 1. Normalized U/Ti ratio in the pH 2.1 buffer solution.

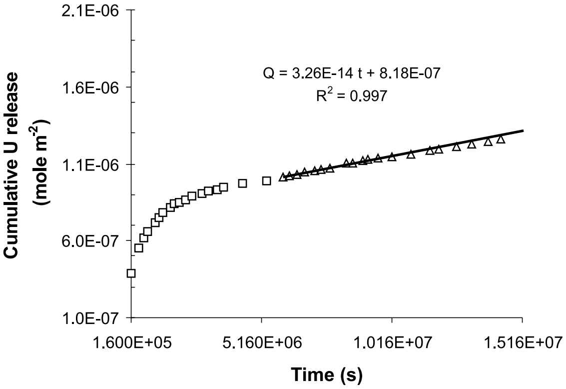

Fig. 2. Plot of U release vs. time for Ce–U ceramic in the pH 5.6 buffer solution at 25°C (flow rate from ~18 to 45 ml d^{-1}).

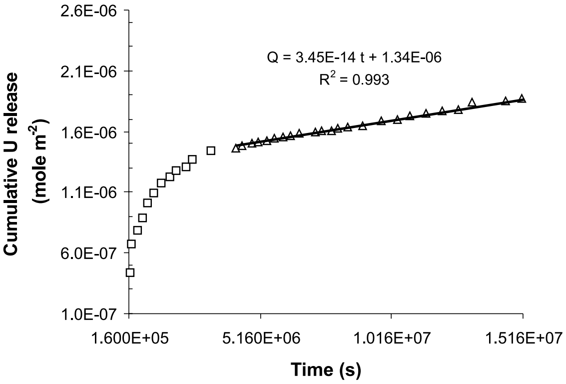

Fig. 3. Plot of U release vs. time for Pu–U ceramic in the pH 5.6 buffer solution at 25°C (flow rate from ~15 to 60 ml d^{-1}).

4. Discussion

4.1. Effect of pH

The dependence of a reaction rate on proton activity is given by

$$R_U = \frac{dQ}{dt} = k_H a^n_{H+}, \qquad (1)$$

where R_U (mol m^{-2} s^{-1}) is the rate of the reaction for U release, k_H (mol m^{-2} s^{-1}) is the apparent rate constant with respect to proton, and n is the order of the reaction with respect to proton activity, which can be determined from the slope ($-n$) of log k vs. pH. The plots of log k (limiting rate constants from Table 4) vs. pH are shown in Fig. 9. The U release rate slightly increases with H$^+$ and OH$^-$ activities with a minimum near pH 8. This suggests that H$^+$ and OH$^-$ promote the U releases to some extent. The fitted reaction orders and log apparent rate constants against H$^+$ are summarised in Table 5.

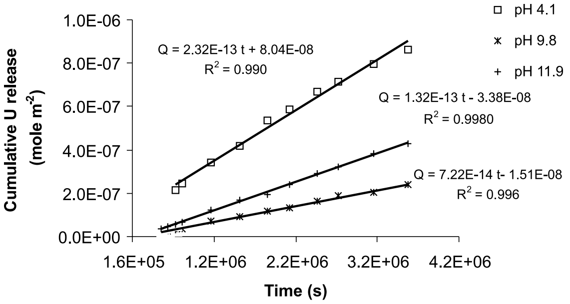

Fig. 4. Plot of U release vs. time for zirconolite in the pH 4.1, 9.8 and 11.9 buffers at 75°C (flow rate from ~40 to 80 ml d^{-1}).

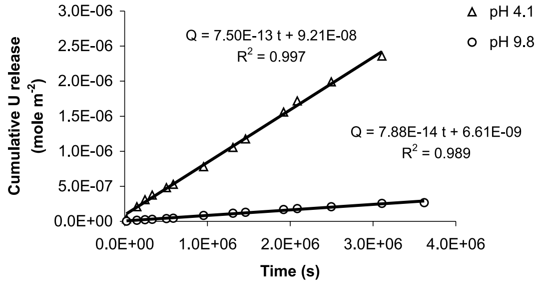

Fig. 5. Plot of U release vs. time for pyrochlore in the pH 4.1 and 9.8 buffers at 50°C (flow rate from ~40 to 80 ml d^{-1}).

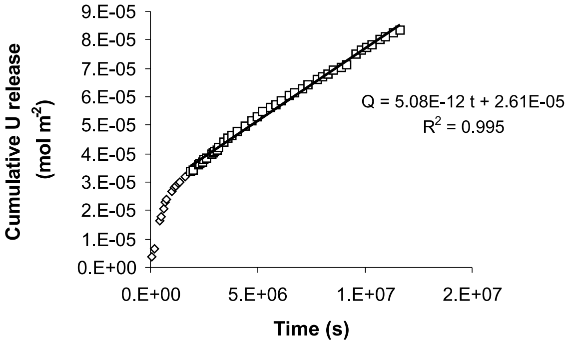

Fig. 6. Plot of U release vs. time for synthetic brannerite in the pH 11.9 buffer solution 70°C (flow rate ~12 ml d^{-1}).

For brannerite there is less pH dependence with a reaction order of 0.16 at pH 2–6 and −0.23 at pH 8–12. The apparent constant is ~1 × 10^{-14} at pH > 8 and ~5 × 10^{-11} at pH < 7. In the case of the other materials, the reaction orders are about −0.20 at pH > 8 and less linear pH dependence at pH < 7 with the reaction orders varying with materials and temperatures from 0 to 0.1 for zirconolite and pyrochlore and 0.2–0.3 for Ce–U and Pu–U ceramics. The apparent constants for H$^+$ remain relatively constant, ~3 × 10^{-16} −3 × 10^{-15} at pH > 8 and ~2 × 10^{-13} −2 × 10^{-12} at pH < 7.

Table 4
Linear ($Q = kt + Q_{\mathrm{o}}$) limiting rate constants for U releases

Solution pH	T (°C)	$K(\pm 2\sigma)$ (mol m^{-2} s^{-1})	Q_{o} (mol m^{-2})
Zirconolite			
2.1	75	$2.43(\pm 0.18) \times 10^{-13}$	2.99×10^{-7}
4.1	75	$2.42(\pm 0.16) \times 10^{-13}$	8.11×10^{-8}
5.6	75	$1.53(\pm 0.02) \times 10^{-13}$	-3.87×10^{-8}
7.9	75	$2.11(\pm 0.05) \times 10^{-14}$	-4.87×10^{-10}
9.8	75	$7.22(\pm 0.28) \times 10^{-14}$	-1.51×10^{-8}
11.9	75	$1.32(\pm 0.03) \times 10^{-13}$	-3.38×10^{-8}
2.1	50	$1.63(\pm 0.20) \times 10^{-13}$	3.51×10^{-7}
4.1	50	$9.04(\pm 1.40) \times 10^{-14}$	4.40×10^{-7}
5.6	50	$8.90(\pm 1.12) \times 10^{-14}$	2.44×10^{-7}
7.9	50	$2.70(\pm 0.20) \times 10^{-14}$	-1.38×10^{-8}
9.8	50	$5.27(\pm 0.26) \times 10^{-14}$	-4.27×10^{-9}
11.9	50	$9.90(\pm 0.94) \times 10^{-14}$	4.00×10^{-7}
7.9	25	$1.25(\pm 0.06) \times 10^{-14}$	8.03×10^{-10}
9.8	25	$2.24(\pm 0.14) \times 10^{-14}$	-4.05×10^{-9}
Pyrochlore			
2.1	75	$1.32(\pm 0.02) \times 10^{-12}$	8.08×10^{-7}
4.1	75	$1.15(\pm 0.09) \times 10^{-12}$	6.03×10^{-7}
5.6	75	$7.02(\pm 0.41) \times 10^{-13}$	-2.97×10^{-7}
7.9	75	$1.58(\pm 0.03) \times 10^{-14}$	6.65×10^{-9}
9.8	75	$1.11(\pm 0.04) \times 10^{-13}$	-4.73×10^{-8}
11.9	75	$1.54(\pm 0.05) \times 10^{-13}$	-2.28×10^{-8}
2.1	50	$9.82(\pm 0.83) \times 10^{-13}$	3.19×10^{-7}
4.1	50	$7.24(\pm 0.19) \times 10^{-13}$	1.13×10^{-7}
5.6	50	$3.71(\pm 0.56) \times 10^{-13}$	2.14×10^{-7}
7.9	50	$3.18(\pm 0.24) \times 10^{-14}$	-9.96×10^{-9}
9.8	50	$7.88(\pm 0.48) \times 10^{-14}$	6.61×10^{-9}
11.9	50	$2.02(\pm 0.29) \times 10^{-13}$	1.28×10^{-7}
4.1	25	$3.70(\pm 0.60) \times 10^{-12}$	2.89×10^{-6}
5.6	25	$5.57(\pm 0.30) \times 10^{-14}$	2.39×10^{-8}
7.9	25	$1.18(\pm 0.10) \times 10^{-14}$	2.96×10^{-9}
9.8	25	$3.32(\pm 0.50) \times 10^{-14}$	-6.69×10^{-9}
11.9	25	$2.10(\pm 0.10) \times 10^{-14}$	7.02×10^{-9}
Brannerite			
2.1	70	$3.59(\pm 0.09) \times 10^{-11}$	2.63×10^{-4}
3.0	70	$9.39(\pm 0.26) \times 10^{-12}$	5.37×10^{-4}
5.6	70	$7.16(\pm 0.52) \times 10^{-12}$	3.56×10^{-4}
7.9	70	$5.62(\pm 0.08) \times 10^{-13}$	8.80×10^{-7}
9.8	70	$7.60(\pm 0.33) \times 10^{-12}$	2.98×10^{-5}
11.9	70	$5.08(\pm 0.11) \times 10^{-12}$	2.61×10^{-5}
5.6	50	$4.38(\pm 0.09) \times 10^{-12}$	8.02×10^{-6}
7.9	50	$5.25(\pm 0.16) \times 10^{-13}$	3.19×10^{-7}
9.8	50	$1.58(\pm 0.02) \times 10^{-12}$	4.03×10^{-7}
5.6	20	$2.97(\pm 0.06) \times 10^{-13}$	4.82×10^{-6}
Ce–U ceramic			
2.1	25	$2.25(\pm 0.18) \times 10^{-13}$	3.02×10^{-6}
4.1	25	$1.11(\pm 0.13) \times 10^{-13}$	1.35×10^{-5}
5.6	25	$3.26(\pm 0.06) \times 10^{-14}$	8.18×10^{-7}
7.9	25	$3.53(\pm 0.10) \times 10^{-14}$	-3.43×10^{-9}
Pu–U ceramic			
2.1	25	$3.50(\pm 0.18) \times 10^{-13}$	3.40×10^{-6}
4.1	25	$1.13(\pm 0.32) \times 10^{-13}$	1.01×10^{-6}
5.6	25	$3.45(\pm 0.11) \times 10^{-14}$	1.34×10^{-6}

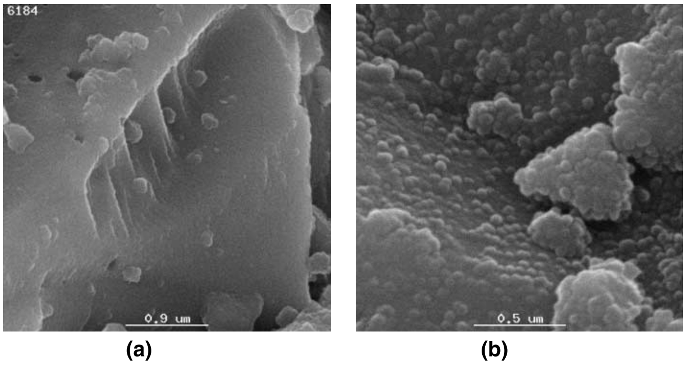

Fig. 7. SEM secondary electron micrographs of the brannerite samples leached in: (a) pH 5.6 buffer for 184 days; (b) pH 11.9 buffer for 156 days.

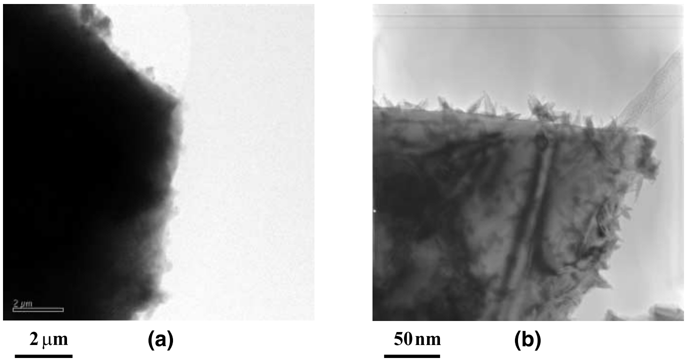

Fig. 8. TEM bright field image of the brannerite sample leached in: (a) pH 5.6 buffer for 184 days; (b) pH 11.9 buffer for 156 days.

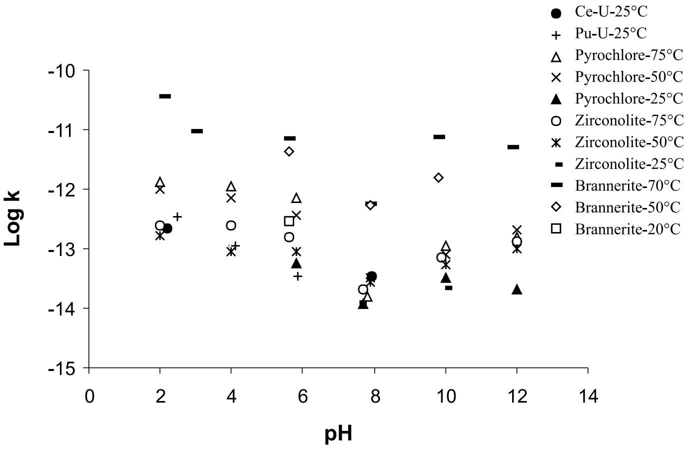

Fig. 9. Plot of log k vs. pH for U release from near single-phase zirconolite, pyrochlore, brannerite, and Ce–U and Pu–U ceramics.

Table 5
Fitted reaction orders and log rate constants with respect to pH

Material	Temperature (°C)	$\log k_H \pm 2\sigma$ pH < 7	$\log k_H \pm 2\sigma$ pH > 8	Reaction order($n \pm 2\sigma$) pH < 7	Reaction order($n \pm 2\sigma$) pH > 8
Zirconolite	70	-12.47 ± 0.29	-15.06 ± 0.68	0.05 ± 0.07	-0.19 ± 0.06
	50	-12.68 ± 0.30	-14.58 ± 0.01	0.07 ± 0.07	-0.13 ± 0.00
Pyrochlore	75	-11.71 ± 0.22	-15.55 ± 1.81	0.07 ± 0.05	-0.24 ± 0.18
	50	-11.76 ± 0.23	-15.05 ± 0.10	0.11 ± 0.05	-0.20 ± 0.01
Ce–U ceramic	25	-12.12 ± 0.28	–	0.22 ± 0.06	–
Pu–U ceramic	25	-11.72 ± 0.04	–	0.30 ± 0.01	–
Brannerite	70	-10.28 ± 0.96	-13.86 ± 3.85	0.16 ± 0.24	-0.23 ± 0.38

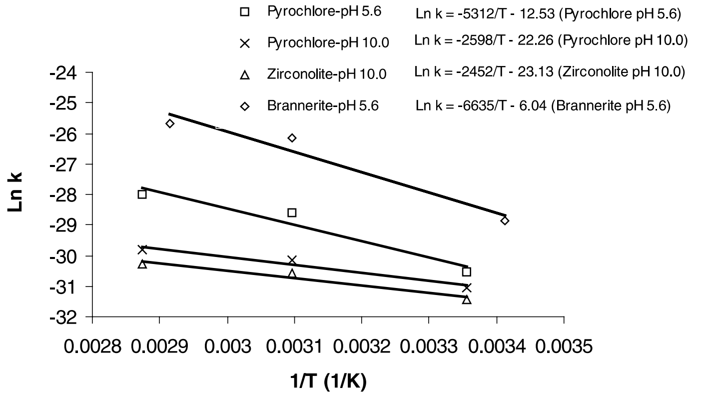

Fig. 10. Plot of Ln k vs. $1/T$ for U release from the near single-phase materials, based on U dissolution rate.

4.2. Effect of temperature

The temperature dependence of a reaction can be expressed by the Arrhenius equation

$$\frac{dQ}{dt} = k = k_T \exp(-Ea/RT), \tag{2}$$

where Ea is the activation energy, R is the gas constant and T is the absolute temperature. The plot of ln k vs. $1/T$ should give a straight line with the slope equal to $-Ea/R$ and from this, the activation energy can be determined.

The plot of ln k (limiting rate constants from Table 4) as a function of inverse temperature (In k vs. $1/T$) gives the activation energies for U releases from pyrochlore, zirconolite and brannerite at different pH values (Figs. 10 and 11). The activation energies based on U data are solely pH dependent (Fig. 11), but do not give the same values as those based on the Ca, Ce and Gd data, implying that the pH dependence is for the U oxidation reaction.

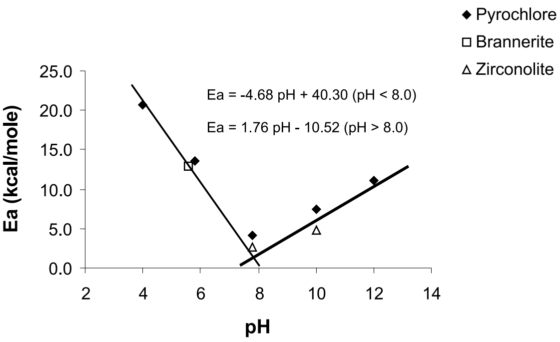

Fig. 11. pH dependence of the activation energy for U release from the near single-phase materials, based on U dissolution rate.

4.3. Mechanism

The initial quick U release (fast surface reaction) followed by a steady state U release (linear kinetics) has been observed. The initial U release process can be viewed as a wetting process – U depletion and formation of a mixed hydroxide layer [18] on the surface, which is largely determined by the temperature, flow rate and pH of the tests, given the same initial surface area. The hydroxide phases formed on the surface control the further U release from the matrix. In the case of brannerite, the preferential U release leaves Ti oxide and hydroxide phases on the surface, which determine the kinetics of further U release from the matrix.

4.4. Comparisons

Based on U releases, zirconolite and pyrochlore have similar reaction rates and rate constant values, which reflects their similar structures [20]. Both of them are more durable (rate constants about 2 orders of magnitude lower) in aqueous media than brannerite. Ce–U (baseline pyrochlore), Pu–U (baseline pyrochlore with impurities) and pyrochlore (near single-phase) samples have closely similar rate constants. There appears to be little effect of including impurity elements on the U releases. In addition, the minor brannerite content of Ce–U ceramic and pyrochlore seems to increase the overall U release rate by only a factor of less than 10.

The dissolution of brannerite exhibits preferential U release leaving behind TiO_2 phases, which is consistent with the alteration rims observed for natural brannerite samples [21]. The close-to-stoichiometric release of U from zirconolite and pyrochlore-rich materials is also in agreement to the fact that U remains relatively less affected by the alteration process in the natural pyrochlore samples [22,23].

5. Conclusions

Zirconolite and pyrochlore-rich titanate materials (pyrochlore, Ce–U and Pu–U ceramics) are more durable in aqueous media than brannerite in the pH range of 2–12. The U releases from these materials are controlled by initial fast process and followed by linear kinetics. The preferential U release from brannerite and close-to-stoichiometric U release from zirconolite and pyrochlore-rich materials are consistent with the observations for the natural samples. For all the materials tested, the U releases vs. pH exhibits a V-shape with a minimum near pH 8. The measured activation energies are solely pH dependent for the near single-phase materials, indicating that the U oxidation probably dominates the overall reaction for U releases from these titanate materials.

Overall, zirconolite and pyrochlore-rich materials are suitable ceramics for actinide immobilisation and are more resistance to aqueous attack than brannerite. However, the impurities and minor brannerite inclusions do not show obvious detrimental effects on U releases from pyrochlore-rich ceramics.

Acknowledgements

The authors wish to acknowledge the partial financial support of this work by USDOE, M.L. Carter for sample preparation and thank E.R. Vance, G.R. Lumpkin, K.L. Smith, V. Mawson and M.W.A. Stewart for helpful discussions.

References

[1] A.E. Ringwood, S.E. Kesson, N.G. Ware, W. Hibberson, A. Major, Nature 278 (1979) 219.

[2] A.E. Ringwood, S.E. Kesson, K.D. Reeve, D.M. Levins, E.J. Ramm, in: W. Lutze, R.C. Ewing (Eds.), Radioactive Waste Forms for the Future, North-Holland, Amsterdam, 1988, p. 233.

[3] E.R. Vance, MRS Bull. XIX (1994) 12.

[4] G.R. Lumpkin, K.P. Hart, P.J. McGlinn, T.E. Payne, R. Giere, C.T. Williams, Radiochim. Acta 66&67 (1994) 469.

[5] G.R. Lumpkin, R.C. Ewing, Am. Mineral. 80 (1995) 732.

[6] E.R. Vance, B. Begg, R.A. Day, C.J. Ball, in: T. Murakami, R.C. Ewing (Eds.), Mat. Res. Soc. Symp. Proc. 353 (1995) 767.

[7] E.R. Vance, A. Jostsons, S. Moricca, M.W.A. Stewart, R.A. Day, B. Begg, M.J. Hambley, K.P. Hart, B.B. Ebbinghaus, Ceram. Trans. 93 (1999) 323.

[8] E.R. Vance, A. Jostsons, R.A. Day, C.J. Ball, B. Begg, P.J. Angel, in: W.M. Murphy, D.A. Knecht (Eds.), Mater. Res. Soc. Symp. Proc. 412 (1996) 41.

[9] A. Jostsons, E.R. Vance, B. Ebbinghaus, Immobilization of surplus plutonium in titanate ceramics, paper presented at Global 99, Jackson Hole, WY, USA, 29 August – 3 September, 1999.

[10] E.R. Vance, J.N. Watson, M.L. Carter, R.A. Day, G.R. Lumpkin, K.P. Hart, Y. Zhang, P.J. McGlinn, M.W.A. Stewart, D.J. Cassidy, Ceram. Trans. 107 (2000) 561.

[11] Y. Zhang, G.R. Lumpkin, A.R. Day, K.P. Hart, S. Leung, M. Collela, M. Carter, Experimental studies of uranium and radionuclides releases from natural brannerites, Migration'99, Lake Tahoe, CA, September–October 1999.

[12] K.P. Hart, E.R. Vance, M.W.A. Stewart, J. Weir, M.L. Carter, M. Hambley, A. Brownscombe, R.A. Day, S. Leung, C.J. Ball, B. Ebbinghaus, L. Gray, T. Kan, in: I.G. McKinley, C. McCombie (Eds.), Mater. Res. Soc. Symp. Proc. 506 (1998) 161.

[13] K.P. Hart, Y. Zhang, E. Loi, Z. Aly, M.W.A. Stewart, A. Brownscombe, B.B. Ebbinghaus, W. Bourcier, Aqueous Durabilities of Titanate Ceramics Designed to Immobilised Excess Pu, Material Research Society Fall Meeting, Boston, MA, 29 November–3 December 1999.

[14] W.L. Bourcier, Interim report on development of a model to predict dissolution behaviour of the titanate waste form in a repository, LLNL, 13 August 1999.

[15] G.R. Lumpkin, K.L. Smith, M.G. Blackford, R. Giere, C.T. Williams, Micron 6&25 (1994) 581.

[16] K.G. Knauss, T.J. Wolery, Geochim. Cosmochim. Acta 50 (1986) 2481.

[17] P.J. McGlinn, K.P. Hart, E.H. Loi, E.R. Vance, in: T. Murakami, R.C. Ewing (Eds.), Mater. Res. Soc. Symp. Proc. 353 (1995) 847.

[18] G. Leturcq, T. Advocat, K. Hart, G. Berger, J. Lacombe, A. Bonnetier, Am. Mineral, to be published.

[19] Y. Zhang, K.P. Hart, R.A. Day, G.R. Lumpkin, M. Colella, P.J. McGlinn, G. Leturcq, B. Thomas, Z. Aly, unpublished material.

[20] K.L. Smith, G.R. Lumpkin, in: J.N. Boland,, J.D. Fitzgerald (Eds.), Defects and Processes in the Solid State: Geoscience Applications, The McLaren Volume, Elsevier, Amsterdam, 1993, p. 401.

[21] G.R. Lumpkin, S.H.F. Leung, M. Colella, Composition, geochemical alteration, and alpha-decay damage effects of natural brannerite, Material Research Society Fall Meeting, Boston, USA, 29 November – 3 December 1999.

[22] G.R. Lumpkin, R.C. Ewing, Am. Mineral. 80 (1995) 732.

[23] G.R. Lumpkin, R.C. Ewing, Am. Mineral. 81 (1996) 1237.